ANALYZING THE EFFICACY AND EXHAUSTS OF PUNNAI BIODIESEL-ETHANOL BLENDS IN NANOCOATED CI ENGINES

Narendranathan Srinivasan Kasinathan[1*], Karthikeyan Subramanian[2], Purushothaman Panneerselvam[1], Srinivasan Tirupathi[2]

[1]Department of Mechanical Engineering, Agni College of Technology, Chennai-600130. Tamil Nadu, India.

[2.]Department of Mechatronics Engineering, Agni College of Technology, Chennai-600130, Tamil Nadu, India.

Received 9.10.2024.
Revised 16.4.2025.
Accepted 9.6.2025.
https://doi.org/10.2298/CICEQ241009015S

[*]Corresponding Author: Email id: sknarengopi@gmail.com, Mobile no +91 7200274636

ABSTRACT

This study experimentally investigates the performance, emission, and combustion characteristics of a nano-coated compression ignition (CI) engine fueled by Punnai biodiesel blends with varying proportions of ethanol. The nano-coating was applied to the engine's cylinder liner and piston crown to enhance heat transfer and reduce friction. The biodiesel blends were prepared by mixing Punnai oil with diesel fuel in various ratios (B20, and B30). Ethanol was added to each blend at 5% and 15% concentrations. This research desires to improve the operational efficiency of an engine which runs on a diesel, through the utilisation of a piston coated with a thermal barrier, specifically tailored for punnai methyl ester blends. Thermal barrier coatings widely prioritise zirconia due to its exceptional thermal insulation properties. B20E15 has a brake thermal efficiency that exceeds that of diesel by around 3%. Similarly, B20E05 and B20E15 demonstrate fuel consumption reductions of approximately 3.8% and 16.3%, respectively. On average, the B20 blends exhibited a reduction in CO and HC emissions are 5% and 9%. A comparative analysis clearly demonstrated that nanocoated CI engines enhance performance and diminish emissions without any major modifications.

Keywords: Punnai biodiesel, ethanol, nano- coating, diesel engine, efficacy, exhausts.

INTRODUCTION

Globally, fuel demand has increased day by day due to logistic infrastructure expansion, fast-growing transport, and high-speed transit [1]. Developing countries rely heavily on fossil fuels as their major mode of transportation. Because of rapid population growth and industrialization, 60% of energy growth will come from fossil fuels. By 2040, it will provide 80% of the world's energy [2]. Although India ranks twenty-first in crude oil production, it holds the third position in terms of crude oil consumption. There exists a substantial disparity between the demand for and production of oil. The observed disparities in crude oil inventory indicate India's significant dependence on imported crude oil [3]. The price of crude oil and growing exhaust gas emissions are the two main things to take into account while utilising diesel as a fuel in an internal combustion engine (ICE) [4]. Transient urban divisions and emissions at the road level present a significant environmental hazard and adversely affect human health. Prolonged exposure can result in the development of lung cancer, asthma, cardiorespiratory disorders, hypersensitivity, and hypertension in humans [5]. The environmental deterioration and significant increase in the usage of fossil fuels underscore the potential of biodiesel as a viable alternative to diesel [6]. This study highlights fuel conversion efficiency and alternatives to diesel. Biodiesel might serve as a feasible fuel for diesel engines owing to its lubricating properties and accessibility. This alternative fuel produces more NOx emissions and possesses a lower calorific value, higher viscosity, and more density compared to diesel. Madhuca indica, Simmondsia chinensis, Calophyllum inophyllum, algae, animal fats, and discarded cooking oils can be utilised to produce biodiesel [7]. Biodiesel has grown in popularity due to its non-toxicity. They have sulphur, oxygen, and a higher cetane number than fossil diesel. Usually, biodiesel emits less than diesel. Biodiesel's lubricity helps engine parts move. One can produce biodiesel using various methods. The process includes first, second, and third-generation feedstock [8].

Traditionally, second-generation biofuels were made from wood residual waste, agricultural waste, and energy crops. Negative or neutral carbon emissions from second-generation biofuels. The seasonal dependence on raw materials is second-generation fuels' biggest drawback [9]. In this study biodiesel production, raw Punnai oil from the kernel of the Punnai tree (Calophyllum inophyllum) is accessible in considerable amounts. Punnai biodiesel yields more oil and heats better than Pongamia, Neem, and Jatropha in Africa and Asia [10]. In addition to the aforementioned benefits, there are notable drawbacks. Use biodiesel exclusively in diesel engines. Biodiesel has consistently shown higher BSFC and NOx emissions compared to fossil fuel, while exhibiting lower BTE and ITE emissions [11]. This study examines the impact of incorporating ethanol into biodiesel-diesel mixtures on the efficiency and exhaust emissions of a CI engine and the results indicate that the incorporation of biodiesel marginally influences engine power at low and medium velocities while enhancing power by around 6% at high velocities. The addition of ethanol greatly improves engine power, with a 16% boost at 1700 rpm and a 13% boost at 2500 rpm for 2.5% and 5% ethanol blends, respectively [12]. The investigation was done on a single-cylinder, four-stroke diesel engine at constant speed under varying loads. These test results optimize the engine load and palm biodiesel/ethanol ratios in diesel-biodiesel-ethanol ternary blends. The research showed that when 11.06% palm biodiesel was used, the best levels of brake thermal efficiency (BTE), nitrogen oxide (NOx), carbon monoxide (CO), and unburnt hydrocarbon (UHC) emissions were at 43.4 percent of capacity. These levels were 12.57 percent, 436.2 parts per million, 0.03 volume percent, and 79.2 parts per million [13]. This study is to assess the effects of nanoparticles in diesel fuel. Different techniques for enhancing engine performance are studied. Nanoparticles are crucial in the advancement of biofuels, from feedstock preparation to chemical reactions. In contrast to blends devoid of alcohol or those with alcohol, whether including nanoparticles or not, the incorporation of nanoparticles into biodiesel-diesel blends decreases brake-specific fuel consumption by 18 to 20 percent. Furthermore, nanoparticles exhibit exceptional heat conductivity, enhancing braking performance by 2% to 5% and optimizing combustion [14].

Further study is being conducted on internal combustion engines with the aim of mitigating expenditure on fuel and maintenance, as well as minimising fuel utilisation. The utilisation of sophisticated ceramic technologies has facilitated implementation of structural modifications as a means to enhance engine efficiency. These coatings were initially observed in gas turbines and aviation engines [14]. In this research, the coatings of ceramics might boost the performance of an engine and lower exhaust by reducing the rejection of heat from cylinder to the cooling system. Utilize the maximum feasible amount of fuel energy. Convert into usable mechanical power. Cover the combustion chamber of an engine to get those results. Newer ceramic materials, which conduct less heat, may increase cylinder temperature and pressure [15]. The nanoparticles have unique physical and chemical properties, including the ability to catalyze reactions, conduct heat, have a higher surface-to-volume ratio, and be more stable because they are so small and move in a Brownian motion. Nanoparticles greatly improve the performance and emissions of current compression ignition (CI) engines by making the combustion process better and breaking up the fuel droplets into small particles. [16]. this research shows that an IC engine with a Nano powder-based thermal barrier coating reduces fuel consumption and increases thermal efficiency. This work reported that the thermal barrier-coated engines increase performance and reduce emissions like HC and CO. NOx emissions increased with combustion temperature [17]. The combustion factors impact output power, pollutants, fuel utilisation, vibration of an engine, and sound. The pressure as well as temperature of air that has been compressed has an impact on the combustion delay. During compression, the cooling and heat-absorbing systems absorb heat. Barrier-coated thermal reduced heat loss can boost engine power. The engine is resistant to high temperatures and has minimal heat conduction. Compounds covering the combustion spaces [18]. Thermal barriers improved thermal and mechanical effectiveness; decreased emissions and lower fuel usage have made engine components popular. Insulation can reduce emissions by oxidizing hydrocarbon combustion soot precursors with engine waste heat [19]. Zirconia coatings on engine components like pistons, inlet and exhaust valves, and cylinder liner have lower heat conductivity. When used in conjunction with a glow plug, ethanol reduces tailpipe emissions but is less fuel-efficient than diesel fuel. Nevertheless, delaying the injection time helps considerably improve the thermal efficiency of the engine. As the combustion temperature rises, the outcome is improved thermal efficiency, reduced emissions of carbon monoxide and unburned hydrocarbons, and increased emissions of nitrogen oxide [20]. Ceramic materials are well-suited for high-temperature applications because of their elevated melting temperatures, robust adhesion, and resilience to wear. Enclosing combustion chamber components is a good application for ceramics. Covered engines provide superior heat retention capabilities within the combustion chamber. Thus, engine emissions and fuel consumption decrease [21]. A study contrasted a nanocoated piston with two coated pistons of different coating thicknesses. The biofuel made a lasting impact. Similar to diesel-fueled trials on coated and nano coated pistons, coating thickness boosts thermal efficiency, fuel consumption, and pollutant reduction [22].

The above research shows that biodiesel reduces greenhouse gas emissions and blends well with diesel. In diesel fuel, biodiesel reduces BTE and increases SFC. Diesel-biodiesel mixed fuel has worse combustion properties than diesel fuel. As biodiesel content increased, NOx emissions rose. A small amount of ethanol can lessen the restrictions on biodiesel-blended fuel. This study explores the impact of ethanol on Punnai biodiesel in 20% and 30% mixes with pure diesel. Nano coating a single-cylinder diesel engine to evaluate its performance and emissions under different load conditions.

EXPERIMENTION AND PROCEDURES

Punnai Oil Source:

The Punnai tree, or Calophyllum inophyllum, is a tropical perennial that thrives in the coastal areas of Southeast Asia, such as India, Sri Lanka, and the Pacific Islands. It holds a special place in Tamil culture due to its robust, long-lasting wood and its various applications in traditional healing practices. The seeds of the tree yield oil that is celebrated for its skin-friendly benefits and possible healing properties. The evergreen C. inophyllum tree has uneven branches and grows to an average height of 8-20 m (25-65 ft). This medium and big coastal tree has 25-mm blooms and elliptical, lustrous, robust leaves. The panicle of this tree contains 4–15 flowers and spherical, green drupes that are 2–4 cm (0.8–1.6 in.) in diameter. Ripe fruit is wrinkled and yellow to brownish-red. Grey, odourless, and ligneous nuts make up the fresh, pale yellow kernel. C. inophyllum kernels yield 50–75% oil, which is useful in medicine and cosmetics. A 3-year-old tree produces approximately 22-100 kg seeds annually. These trees generally live approximately 50 years and are located in mild to warm Indian Sea coastal locations. They are prevalent in 1000–5000 mm rainfall zones.

Availability of Punnai Bio-oil and its impact in IC Engine:

Punnai trees (Calophyllum inophyllum) are common in coastal India, especially in Tamil Nadu, Kerala, and Andhra Pradesh, where their seeds are used for medical purposes. Punnai seed oil seems promising as a biofuel for internal combustion engines. Many biodiesel manufacturing advantages come from these seeds' oil. Furthermore, its high oxidative stability inhibits oil degradation, extending shelf life and improving engine performance. Punnai oil offers an environmentally beneficial alternative to diesel due to its low sulphur level. Due to its diesel-like viscosity, Punnai oil's lubricity reduces engine wear and enables its use in I.C. engines without any modifications. Punnai's oil biodiesel contains a higher cetane number, which improves engine performance and fuel efficiency. Punnai seed oil lowers carbon emissions and fossil fuel use by providing renewable energy. Punnai oil's technical merits and popularity in India might help the country promote sustainable energy and reduce environmental effects. Figure 1 (a) shows oil extraction process of punnai bio-oil.

Novelty of Punnai oil Utilization:

The technical novelty of using Punnai oil (Calophyllum inophyllum) as a biodiesel source is attributed to its distinctive fatty acid composition, elevated free fatty acid levels, and advantageous fuel characteristics. The composition necessitates a two-step transesterification process that, when optimised, produces biodiesel with a high cetane number (>50), flash point (>160°C), and density (0.87–0.89 g/cm^3) compliant with ASTM requirements. Notwithstanding somewhat increased viscosity, it provides enhanced lubricity, superior combustion quality, and oxidative stability. Punnai biodiesel, which has a heat value of 38–41 MJ/kg, is suitable for diesel engines, making it a practical, non-food, and sustainable source for biodiesel.

GC-MC Analysis of Punnai Bio-Oil

The produced sample underwent purification for Punnai biofuel through the process of distillation. The level of bio-oil was determined through gas chromatography (Thermo Scientific), equipped with a flame ionization detector (FID). The setup included a TG-Wax MS column with a length of 30 m, an internal diameter of 0.25 mm, and a film thickness of 0.25 µm. The oven's temperatures increased steadily at a rate of 7°C per minute, starting from 40°C and reaching 180°C. Meanwhile, the injector was kept at 230°C, and the detector was maintained at 250°C. Before injecting into GC, samples were filtered using 0.22 µm syringe filters. The high-purity nitrogen served as the carrier gas, while the flask generated zero air and hydrogen gases. Figure 1(b) and Table 1 show the retention time in minutes along the x-axis and the range of potential ethanol sources on the y-axis. The retention time of biofuel produced from Punnai seed oil is 2.59 minutes, suggesting that the standard time for bio-oil production closely aligns with the actual retention time observed.

Free Fatty Acid Composition:

The composition of fatty acids Gas chromatography analysed the free fatty acid content of Punnai's oil biodiesel, as seen in Figure 1 (c) and table 2. Punnai oil biodiesel/methyl ester has 24% saturated methyl esters and 76% unsaturated methyl esters. Punnai oil contains a significant concentration of unsaturated fatty acids, with 34.29% oleic acid and 41.711% linoleic acid. These unsaturated fatty acids improve cold flow and combustion efficiency, while linoleic concentration may diminish oxidative stability. Palmitic acid (C16:0) is the most common saturated fatty acid at 14.878%, while stearic acid (C18:0) adds 6.226%, increasing biodiesel cetane number and storage stability. In tiny doses, 0.523% and 0.428% of lauric acid (C12:0) and myristic acid (C14:0) promote lubricity. Linolenic acid (C18:3), at

0.069%, is extremely unsaturated and oxidative, which improves fuel stability. With a balanced blend of saturated and unsaturated fatty acids, Punnai oil-derived biodiesel should meet fuel standards for ignition quality, viscosity, and oxidative stability.

TABLE 1 INSERT HERE

FTIR:

The vibrational approach Fourier transform infrared spectroscopy (FTIR) finds organic compounds on biofuel surfaces. It helps qualitatively evaluate materials and comprehend organic groupings [37]. The Perkin Elmer spectrum two FTIR analyser identified chemical bonds, functional groups, and the vibrations of Punnai oil (eitherbending or stretching). FTIR examined Artocarpus heterophyllus peel biofuel. Figure 1(c) presents the FTIR spectrum data for the biodiesel sample, with the wavenumber (cm-1) plotted against transmittance (%). Table 4 displays the measurements from the Perkin Elmer machine of functional group vibrations (500-4000 cm^{-1}) for solids and liquids, including amide, aldehyde, alkyl, ester, anhydride, phenolic, carboxylic, ketonic, and many other vibrations.

TABLE 2 INSERT HERE

Test Sample and its Properties

The current study seeks to examine the effects of adding ethanol to nanocoated pistons powered by Punnai biodiesel. The study involved blending biodiesel from the Punnai seed biodiesel transesterification process with diesel fuel at varying volume ratios of 20% and 30%. Additionally, we added oxygenated ethanol additives at concentrations of 5% and 15%. The fuel for the nanocoated engine (NCE), known as B20E05, is a blend of 20% Punnai biodiesel (B20), 5% volumetric ethanol, and 75% pure diesel. Formulate the biodiesel fuel blends as follows: B20E15, which is 65% diesel, 20% Punnai biodiesel, and 15% ethanol; B30E05, which is 65% diesel, 30% Punnai biodiesel, and 5% ethanol; and B30E15, which is 55% diesel, 30% Punnai biodiesel, and 15% ethanol. Table 3 displays the test sample's properties.

FIGURE 1 INSERT HERE

TABLE 3 INSERT HERE

Test Engine and Facilities

Figure 1 shows the design of a compression ignition engine with attached instrumentation, where the prepared test fuel undergoes testing. Table 4 lists engine specs. Water-cooled eddy current dynamometers are powered by engines on base frames with universal propeller shafts. The sensors are installed at acceptable places and linked to the engine test panel to display engine torque and speed, which are utilised to calculate braking power. A high-speed digital data collection system collected pressure and TDC signals, which were stored on a computer to calculate engine combustion parameters. The AVL Digas 444 analysed NOx, HC, CO, and CO_2 exhaust pollutants. The opacity of smoke was calculated with the help of AVL 437C smoke gauge.

FIGURE 2 INSERT HERE
TABLE 4 INSERT HERE

Error Analysis

This section, the errors linked to the different metrics, was calculated using the approach proposed by **[31].** We computed the associated errors for the lowest possible values of the instrument's output and quality. To get the margin of error for an estimated quantity S that is dependent on a set of independent variables (x1, x2, x3… xn), one can use equation (1).

$$\frac{\partial S}{S} = \left\{ \left(\frac{\partial X_1}{X_1}\right)^2 + \left(\frac{\partial X_2}{X_2}\right)^2 + \cdots + \left(\frac{\partial X_n}{X_n}\right)^2 \right\}^{\frac{1}{2}} \qquad \text{------------- (1)}$$

The experimental minimum value of the output is denoted by X1, and the errors in the independent variables ∂X_1 with respect to the measuring instrument's precision are denoted by $\left(\frac{\partial X_1}{X_1}\right)$,$\left(\frac{\partial X_2}{X_2}\right)$, etc.

BTE and SFC calculation errors maxed out at 0.38 %. Cylinder pressure and crank angle errors were 0.25 and 2%, respectively. Analyser specs allow for a maximum error of 5% in measuring smoke opacity and NO_x emission.

Test procedure

Initially, the experiment was conducted in controlled environmental conditions using Punnai biodiesel and diesel blend (B20) in an unmodified engine. Prior to each observation, the engine was run for a period of 5 minutes to generate a condition of equilibrium. Moreover, the experiments were carried out by incorporating ethanol at volumes of 5% and 15% into the diesel fuel. The ideal blend was determined to be B20%, with a compression ratio of 17.5. The injection time was set at 23° bTDC. The test results were arranged in ascending order of load, ranging from 25% to 100%. The engine trials will be conducted using four specific test fuels, namely: (1) diesel fuel, (2) B20E05 (20% biodiesel + 5% ethanol), (3) B20E15 (20% biodiesel + 15% ethanol), (4) B30E05 (30% biodiesel + 5% ethanol), and (5) B30E15 (30% biodiesel + 15% ethanol). Experimental investigations were conducted on a nanocoated DI-CI engine, maintaining consistent operating conditions at the designated power output. These tests were conducted on a single day and in ecologically comparable environments. The main motive of this study is to improve the efficiency, reduce the NOx and smoke emissions through minor modifications to the engine's characteristics. In contrast to the author's prior study, which employed the identical ternary blend without making any engine adjustments, the current study yielded reduced efficiency and increased smoke emissions when compared to synthetic diesel fuel.

OUTCOMES AND ANALYSIS

FIGURE 3 INSERT HERE

Combustion Analysis

CP:

Cylinder pressure (CP) is the peak pressure that may be achieved within the combustion zone, following complete burning of the fuel. Figure 3 (a) shows the cylinder pressure of different fuel mixtures as the engine load increases. Because there are more fuel oxygen molecules in biodiesel, it burns more efficiently. This means that the pressure in the combustion chamber rises faster than with regular diesel. [32]. Moreover, the use of ethanol in biodiesel blends (E05 & E15) enhances cylinder pressure, especially evident at elevated engine loads. There are a lot of things that point to this conclusion. For example, ethanol has a higher autoignition temperature and more heat when it evaporates. Biodiesel has a higher pressure when mixed with ethanol in the cylinder, and it releases more heat than biodiesel. Biodiesel blends with ethanol perform better than biodiesel blends with diesel fuel when it comes to increasing cylinder pressure and rate of pressure [33].

HRR:

The most crucial combustion factor in a diesel engine is the cylinder heat release rate (HRR). One definition of HRR is the quantity of heat that an energy source may generate in a given length of time. The pressure within the cylinder and the pace at which it is increasing to its peak are the two variables that affect the heat transfer rate. [34]. There were consistent trends with respect to crank angle in the biodiesel and diesel HRRs. Figure 3 (b) clearly shows that the biodiesel trajectory has moved to the left compared to the diesel trajectory. This means that combustion happens faster in biodiesel–diesel blends than in base diesel. An increase in HRR was noted when the ethanol % rose in comparison to blended fuel. This might be because of the faster heat release followed by better mixture preparation during the delay period. The highest peak of premixed combustion HRR is observed in the fuel that is blended with ethanol, suggesting that a greater percentage of the fuel is burnt during this phase [35].

Performance Characteristics

FIGURE 4 INSERT HERE

Brake thermal efficiency (BTE)

Figure 4 (a) depicts a different fuel blend can perform differently in terms of BTE, Biodiesel and ethanol blend of B20E15 showed a 2-3% higher BTE than pure diesel under maximum load. The higher oxygen concentration in ethanol enhances the efficiency of combustion. As a result of the high ethanol content in the mix, the viscosity and combustion rate are lower; therefore the BTE is lower than B30E15. The density and viscosity of punnai biodiesel are higher than diesel, which causes the first combustion phase to be slower and the BTE to decrease compared to diesel [10]. The blend density is increased by high levels of latent heat and volatility from ethanol, which in turn improves the brakes' thermal efficiency as the ethanol proportion increases. The temperature of the air-fuel combination drops, as the amount of ethanol in the mixture rises, leading to better premixed combustion, since the air temperature in the emulsion is lower and there is a longer period of time for the fire to start because of the lower temperature in the air [23]. As a result of the coating of ceramic acts as a heat shield separating the engine from its surroundings, the engine with partially stabilized zirconia coating has a low heat rejection achieved a much enhanced thermal efficiency in comparison to the other engines based on the fact that the coating of ceramic acts as a heat shield. By reducing heat loss, it is possible to increase the power and thermal efficiency of an engine [20].

Specific fuel consumption (SFC)

Fuel injection increases as engine load rises, resulting in a higher SFC ratio. Figure 4 (b) shows the SFC with engine load and ethanol ratios, indicating that the SFC reduces as the engine load increases. There was a 3.8 % decrease in SFC for B20E05 blend and 16.3%

decrease for B20E15 blend when correlated to diesel, respectively. Fuel consumption was 9% higher with B30E15 blends correlated to diesel, however. Due to the lower calorific value of biodiesel blends and the higher density, biodiesel blends require more fuel to run an engine than conventional diesel. Increasing the biodiesel blend ratio leads to higher fuel consumption since it decreases the fuel mixture's density and calorific value [24]. Study results indicate that the coating provides superior heat retention, which results in higher temperatures inside the cylinders. Temperature increases in the cylinder improves the biofuel mix's oxidation, which results in the better atomization. Improved atomization and vaporization reduce consumption of fuel while maintaining speed of engine [17].

Equivalence Ratio ((λ)

The air-to-fuel equivalence ratio (λ) was measured at full engine power for different fuel mixtures, including pure Diesel (D100) and blends of Punnai biodiesel and ethanol. The engine operated at a compression ratio (CR) of 17.5:1, which is typical for CI engines [36]. At full load, the equivalence ratio (λ) indicates how lean or rich the air–fuel mixture is compared to the stoichiometric ideal, where a λ value greater than 1 denotes a lean mixture (excess air), and a value less than 1 indicates a rich mixture. Among all tested fuels, pure diesel exhibited the highest λ value of 1.724, indicating the leanest combustion. The B20E15 blend followed closely with a λ of 1.722, suggesting similarly efficient combustion. B20E05 and B30E05 showed slightly richer mixtures, with λ values of 1.664 and 1.674, respectively. B30E15 recorded the lowest λ value of 1.459, indicating the richest mixture among the samples. Overall, all fuel blends operated under lean conditions, with diesel and B20E15 demonstrating optimal air utilisation.

Emission Characteristics

FIGURE 5 INSERT HERE

Nitrogen oxide (NOx)

Nitrogen oxide (NOx) emissions can be reduced by reducing the premixed burning rate, while releasing heat at a slower rate. In ethanol biodiesel dual-fuel engines, NOx emissions rise with the increase in ethanol's energy share. A number of factors influence NOx generation [23]. The sudden rise in NOx emissions was attributed to increased engine load in the presence of higher fuel consumption. As a result, NOx emissions decreased [21]. It is shown in figure 5 (a) that at full load circumstances, B20E05, B2015, B30E05, and B30E15 fuels shows higher NOx concentrations than diesel, at rates of 3.8%, 4.6%, 5.4%, and 13.9%, respectively. However, one aspect of the coated engine requires attention, and a result has demonstrated that coated piston engines emit more NOx than uncoated piston engines. It may also be that the temperature of the NOx emissions is higher, thus resulting in an earlier ignition, which transfers pressure and temperature in a less efficient manner. A coated piston engine emits more NOx than a nanocoated piston engine. The higher temperature and pressure in the combustion process may cause the engine to emit more NOx, resulting in higher emissions. The majority of biofuels are burned in the premixing phase before combustion, so NOx levels are reduced during combustion [19].

Smoke Opacity (SO)

The figure 5 (b) shows a trend in smoke release to enhancing smoke reduction in engines involves two crucial elements: elevating the combustion chamber temperature and minimising heat transfer to the coolant. Due to the high combustion chamber temperature, nanocoating can enhance evaporation by increasing the proportion of premixed fuel in the chamber of combustion. Thus, the diffusion burn is lowered, which reduces the generation of smoke as a result [26]. At maximum load conditions, the smoke generation rates increases for the biodiesel and ethanol blends when correlating to diesel. The blends B20E05, B2015, B30E05, and B30E15 produces the smoke levels of 12%, 3.8%, 13.3%, 10%, and 14.9% higher than diesel, respectively. If the fuel is burned inefficiently, smoke is produced. A reduction in smoke emissions is also influenced by the reduction in latent heat of vaporization and the ignition delay that occur with increasing load of the engine[27]. The application of nanocoated on engine components results in an increased heat retention rate inside the cylinder, which is completely capable of burning the fuel. As a result, coated engines reduce their smoke emissions.

Carbon monoxide (CO)

Figure 5 (d) depicts the influence of different biodiesel mixes on the release of carbon monoxide (CO). At low loads, diesel emits less CO than biodiesel blends when full combustion occurs. As a result of chemical processes that allow CO production to be enhanced, biodiesel blends emit less CO, but more CO_2 as a result of greater oxygen content [28]. Compared with pure diesel, B20E05 and B20E15 blends reduce CO concentrations by 5.8% and 8.6%, respectively, whereas B30 blends increase the amount of CO emissions. Additionally, thermal barrier coatings on engines significantly decreased the amount of CO that was emitted, with coated engines emitting significantly less CO than uncoated engines. Thermal insulation that has been coated with nanoparticles is activated by combustion in the late phase and the oxidation of CO, which results in a reduction in CO concentrations as the speed of the combustion increases. As long as the engine operates at its optimal speed, CO emissions are almost negligible, indicating that CO emissions are substantially controlled independent of piston coating [29].

Hydrocarbon (HC)

Figure 5 (c) shows the hydrocarbon exhausts. The oxidation of atmospheric hydrocarbons with oxygen in ethanol improves fuel efficiency, reducing hydrocarbon (HC) emissions. The oxidation of hydrocarbons during combustion can be enhanced by ethanol, an alcohol with oxygen. Combined with biodiesel, ethanol can reduce HC emissions and increase fuel efficiency [7]. As a result of the higher combustion pressure and temperature caused by ethanol combustion, hydrocarbons are more completely oxidized. However, hydrogen lead combustion in diesel engines produces lower combustion pressure and temperatures, leading to lower oxidation of hydrocarbons and higher emissions of HC as a result of lower pressure as well as temperature during combustion [25]. According to the findings of the study, the hydrocarbon emissions of B20E05 and B20E15 blends were reduced by 2.5% and 8.6%, respectively, when compared to pure diesel. On the other hand, the hydrocarbon emissions of B30E15 blends were raised by 10% when compared to diesel. A thermal barrier layer was employed to raise combustion temperature in the study to improve fuel combustion. Because hydrocarbons break down faster as hydrogen and oxygen in the chamber of the combustion, the thermal barrier layer reduced hydrocarbon emissions. Hydrocarbon emissions cause air pollution and threaten human health, thus reducing them is crucial. A heat barrier coating must be examined together with quenching distance and flammability threshold, which are safety factors. The study also shows how ethanol mixes affect fuel usage, carbon monoxide emissions, hydrocarbon emissions, and nitrogen oxide emissions [30].

The limitations of using biodieel are listed below,

1. The accessibility and expense of biodiesel feedstocks can be affected by variables such as land accessibility.
2. Compared to oil-based diesel, biodiesel now has a limited production capacity.
3. Biodiesel may exhibit elevated cloud point and pour point temperatures relative to petroleum diesel, potentially impacting its flow and performance under cold weather

situations. Incorporating petroleum diesel or other additives might mitigate this problem.

4. Biodiesel has worse oxidative stability compared to petroleum diesel, rendering it more susceptible to deterioration and sediment development over time.

CONCLUSIONS

Emerging economies like India widely use diesel-powered vehicles to transport commodities and people. Traffic, fuel use, and environmental hazards rise. Plant-based biofuels, such as diesel, may solve these problems. This study aims to examine diesel engine performance with ethanol-biodiesel mixes generated from punnai seed. A nanoparticle-covered single-cylinder diesel engine burnt biodiesel and ethanol in different proportions to optimise combustion.

- Ethanol-blended biodiesel (E05 & E15) increases cylinder pressure, particularly under high engine loads, owing to improved combustion efficiency and elevated heat release. These mixes surpass conventional diesel and biodiesel in enhancing cylinder pressure.
- The brake efficiency of engines B20E15 exhibits a 3% improvement compared to diesel. With regards to B20E05 and B20E15, ethanol contains a significantly higher concentration of oxygen compared to diesel.
- The comparison of the specific usage of these two fuel types reveals a reduction of approximately 3.8% and 16.3% in consumption of fuel, respectively.
- The combustion emissions of NOx from the ideal B20E05 mixture exhibit an average reduction of 13.13% compared to the emissions seen in other test samples.
- The CO and HC emissions went down ranging from 5% and 9% with the B20 blends.
- Finaly, operating at maximum load, the B20E15 exhibits optimal levels of CO and HC emissions, measuring at 0.3% and 56 ppm, respectively. Additionally, it achieves a fuel consumption of 0.321 kg/kWh.

REFERENCES

[1] I. Veza, A.D. Karaoglan, E. Ileri, Case Stud. Therm. Eng. 31 (2022) 101817. https://doi.org/10.1016/j.csite.2022.101817

[2] A.T. Hoang, S. Nižetić, H.C. Ong, W. Tarelko, V.V. Pham, T.H. Le, M.Q. Chau, X.P. Nguyen, Sustainable Energy Technol. Assess. 47 (2021) 101416. https://doi.org/10.1016/j.seta.2021.101416

[3] B. Sharma, A. Shrestha, Energy Strategy. Rev. 45 (2023) 101053. https://doi.org/10.1016/j.esr.2023.101053.

[4] Y. Devarajan, R. Jayabal, D.B. Munuswamy, S. Ganesan, E.G. Varuvel, Process. Saf. Environ. Prot. 165 (2022) 374–439. https://doi.org/10.1016/j. psep.2022.07.001

[5] M. Çelik, C.Bayındırlı, M.Mehregan, Environ. Sci. Pollut. Res. 29 (2022) 30277–30284. https://doi.org/10.1007/s11356-021-18012-1

[6] M.N. Bin Mohiddin, Y.H. Tan, Y.X. Seow, J. Kansedo, N. Mubarak, M.O. Abdullah, Y.S. Chan, M.J. Khalid, Ind. Eng. Chem. 98 (2021) 60–81. https://doi.org/10.1016/j.jiec.2021.03.036

[7] R. Sathyamurthy, D. Balaji, S. Gorjian, S.J. Muthiya, R. Bharathwaaj, S. Vasanthaseelan, Sustainable Energy Technol. Assess. 43 (2021) 100981. https://doi.org/10.1016/j.seta.2020.100981

[8] P. Łagowski, G. Wcisło, D. Kurczyński, Energies 15 (2022) 6835. https://doi.org/10.3390/en15186835

[9] Y. Devarajan, R.K. Jayabal, D. Ragupathy, H. Venu, Front. Environ. Sci. Eng. 11 (2017) 1-6. https://doi.org/10.1007/s11783-017-0891-0.

[10] B. Chidambaranathan, P. Seenikannan, P. Seenikannan. J. Therm. Sci. 24 (2020) 13-25. https://doi.org/10.2298/TSCI180325233B

[11] K. Subramanian, S.A. Paramasivam, D. Dillikannan, M. Muthu, P.R. Yadav Sanjeevi, Int. J. Ambient Energy (2022) 1–14. https://doi.org/10.1080/01430750.2022.2103184

[12] F.Hamdi, I. Yahya, M. Gassoumi, Z. Boutar, R.M.R. Ahsan Shah, M. Al. Qubeissi, R.Ennetta, and H. S. Soyhan. Sci. Tech. Energ. Transition, 33 (2024). https://doi.org/10.2516/stet/2024033

[13] S.Dey, A.P.Singh, S.S. Gajghate, S.Pal, B.B .Saha, M. Deb, P.K. Das. Sustainability. (2023) 15(20):14667. https://doi.org/10.3390/su152014667

[14] M. Nagappan & J. M. Babu. Mater. Today: Proc., (2023) https://doi.org/10.1016/j.matpr.2023.01.122

[14] L. Urtekin, S. Bayaşoğlu, Surf. Rev. Lett. 27 (2020) 1950158. https://doi.org/10.1142/S0218625X19501580

[15] D. Sakthivadivel, P.G. Kumar, R. Prabakaran, V. Vigneswaran, K. Nithyanandhan, S.C. Kim, Case Stud. Therm. Eng. 34 (2022) 102021. https://doi.org/10.1016/j.csite.2022.102021

[16] M. Tomar, N. Kumar, Energy Sources, Part A (2019) 1–18. https://doi.org/10.1080/15567036.2019.1623347

[17] P. Kumaran, S. Natarajan, IOP Conf. Ser.: Mater. Sci. Eng. 993 (2020) 012014. https://iopscience.iop.org/article/10.1088/1757-899X/993/1/012014/pdf.

[18] M.M. Musthafa, Int. J. Sustainable Energy Eng. 11 (2018) 159–166. https://doi.org/10.1080/19397038.2017.1393024

[19] M. Selvam, S. Shanmugan, S. Palani, Environ. Sci. Pollut. Res. 25 (2018) 35210–35220. https://doi.org/10.1007/s11356-018-3419-7

[20] P. Balu, P. Saravanan, V. Jayaseelan, Mater. Today: Proc. 39 (2021) 1259–1264. https://doi.org/10.1016/j.matpr.2020.04.160

[21] V. Dananjayakumar, M.B. Sanjeevannavar, S.M. Golabhanvi, M.A. Kamoji, Mater. Today: Proc. 42 (2021) 1387–1392. https://doi.org/10.1016/j.matpr.2021.01.113

[22] A.M. Narad, M.P. Joshi, Results Mater. 8 (2020) 100140. https://doi.org/10.1016/j.rinma.2020.100140

[23] L. Geng, L. Bi, Q. Li, H. Chen, Y. Xie, Energy Rep. 7 (2021) 904–915. https://doi.org/10.1016/j.egyr.2021.01.043

[24] S.B. Sai, N. Subramaniapillai, M.S.B. Khadhar Mohamed, A. Narayanan, Fuel 296 (2021) 120708. https://doi.org/10.1016/j.fuel.2021.120708

[25] V.E. Geo, A. Sonthalia, G. Nagarajan, B. Nagalingam, Fuel 209 (2017) 733–741. https://doi.org/10.1016/j.fuel.2017.08.036

[26] J. Kumaraswamy, V. Kumar, G. Purushotham, R. Suresh, J. Therm. Eng. 7 (2021) 415–428. https://doi.org/10.18186/thermal.882965

[27] S.R.K. Valiveti, H. Shaik, K.V.K. Reddy, Int. J. Ambient Energy (2020) 1–18. https://doi.org/10.1080/01430750.2020.1831592

[28] K. Sudalaiyandi, K. Alagar, R. Vignesh Kumar, V.J. Manoj Praveen, P. Madhu, Fuel 285 (2021) 119255. https://doi.org/10.1016/j.fuel.2020.119255

[29] N. Ramasamy, M.A. Kalam, M. Varman, Y.H. Teoh, Coatings 11 (2021) 692. http://eprints.um.edu.my/id/eprint/26425

[30] S. Padmanabhan, C. Joel, L. Joel, O.Y. Reddy, K.G.D.S. Harsha, S. Ganesan, Nat. Environ. Pollut. Technol. 20 (2021) 2079–2086. https://doi.org/10.46488/NEPT.2021.v20i05.025

[31] A. Naresh Kumar, P.S. Kishore, K. Brahma Raju, K. Nanthagopal, B. Ashok, Fuel 276 (2020) 118076. https://doi.org/10.1016/j.fuel.2020.118076

[32] D. Balasubramanian, A.T. Hoang, I.P. Venugopal, A. Shanmugam, J. Gao, T. Wongwuttanasatian, Fuel 287 (2020) 119815. https://doi.org/10.1016/j.fuel.2020.119815

[33] K.R.Kavitha, J. Jayaprabakar, A.Prabhu, Int. J. Ambient Energy 43 (2019) 778–782. https://doi.org/10.1080/01430750.2019.1670261

[34] A.F.Emma, S.Alangar, A.K.Yadav, Energy Convers. Manage: X 14 (2022) 100214. https://doi.org/10.1016/j.ecmx.2022.100214

[35] S. Rajendran, M. Govindasamy, Energy Sources, Part A (2021) 1–16. https://doi.org/10.1080/15567036.2021.1887408

[36] Shanmugam, R., Dillikannan, D., Kaliyaperumal, G., De Poures, M. V., & Babu, R. K, .Energy Sources, Part A (2020) 43(23), 3064–3081. https://doi.org/10.1080/15567036.2020.1833112

[37] K. Subramanian, S.A. Paramasivam, D. Dillikannan. J. Ravikumar, Sustainable Energy Technol. Assess. 58 (2023) 103345. https://doi.org/10.1016/j.seta.2023.103345

Figure Captions

Figure 1 (a) Punnai Oil extraction, (b) GC-MS Analysis (c) FTIR Analysis

Figure 2 Schematic layout of Test Engine setup

Figure 3 (a) CP (b) HRR (vs) different load conditions

Figure 4 (a) BTE (b) SFC (vs) different load conditions

Figure 5 (a) NOx, (b) Smoke (c) HC and (d) CO for (vs) different load conditions

Table 1 GC-MS analysis

Fatty Acids	Formula	Systematic name	Retention Time
Lauric acid	$C_{12}H_{24}O_2$	Dodecanoic acid (C12)	21.48
Myristic acid	$C_{14}H_{28}O_2$	Tetradecanoic acid (C14)	26.76
Palmitic acid	$C_{16}H_{32}O_2$	Hexadecanoic acid (C16)	15.68
Stearic acid	$C_{18}H_{38}O_2$	Octadecanoic acid (C18)	18.00
Oleic acid	$C_{18}H_{34}O_2$	Cis-9- Octadecanoic acid (C18:1)	26.54
Linoleic acid	$C_{18}H_{32}O_2$	Cis-9-cis12-Octadecanoicacid (C18:2)	22.14
Arachidice acid	$C_{20}H_{40}O_2$	Eicosanoic acid (C20)	27.13
Behenic acid	$C_{22}H_{44}O_2$	Docosenoic acid (C22)	24.06

Table 2 Functional group based FTIR

Wave Number (cm^{-1})	Experimental Results (cm^{-1})	Organic Groups and Their Nature	Chemical Formation
3100–3500	3453, 3477, 3476	O–H & Stretching	Alcoholic, Phenolic
2800–3000	3453, 3477, 3476	O–H & Stretching	Alkanes
1680–2700	1750, 1745, 2027	C–H & Bending	Aromatic
1250–1650	1625, 1469, 1456	C=C & Stretching	Alkenes
1200–1000	1170, 1164, 1105	C–O & Stretching	Ester
1000–500	776, 728, 721	COO & Stretching	Carboxylic

Table 3 test sample's properties

Properties	ASTM Standard	Diesel	Punnai Biodiesel	Ethanol	Instrumentation
Kinematic viscosity (at40°C) (cst)	D 445	2.42	4.88	1.52	Red Wood viscometer
Density at15°C (kg/m^3)	D 941	830	867	720	Hydrometer
LHV (MJ/kg)	D 240	42.5	40.39	26.92	Bomb Calorimeter
HHV (MJ/kg)		45.5	42.31	29.7	
Cetane Index	D 613	54	49	10	Ignition Quality Tester
Flash point (°C)	D 93	58	165	13	Pensky Martins Apparatus

Table 4 Engine specifications

Make and Model	**Kirloskar, TV1**
Number of cylinders/Stroke	One/Four
Bore x Stroke	87.5 x 110 mm
Compression ratio	17.5:1
Swept volume	661cc
Maximum power output	5.2 kW at 1500rpm
Lubricating oil	SAE40
Cooling system	Water cooled
Injection pressure	210 bar
Standard Injection timing, CA bTDC	23°

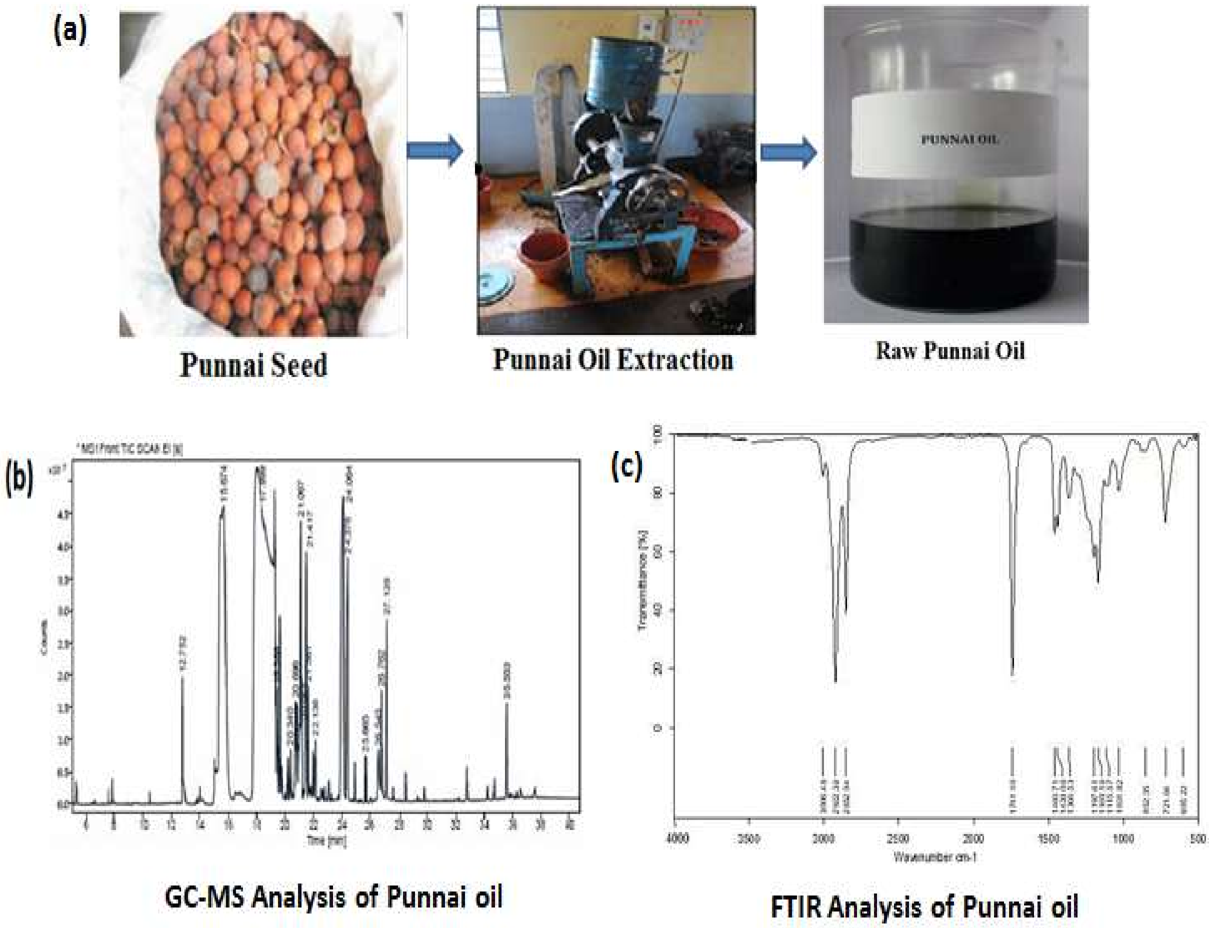

(a)
Punnai Seed
Punnai Oil Extraction
PUNNAI OIL
Raw Punnai Oil
(b)
GC-MS Analysis of Punnai oil
(c)
FTIR Analysis of Punnai oil

Figure 1

Nano-coating piston mounted in cylinder head

Test Engine Setup

Figure 2

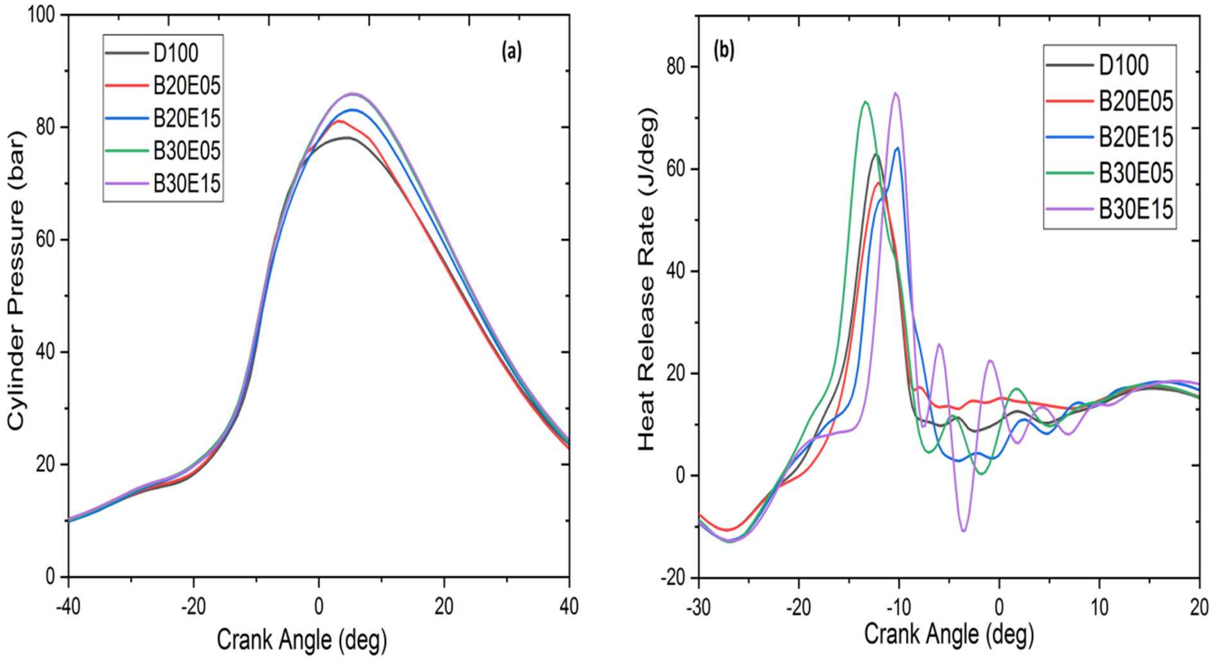

(a)
D100
B20E05
B20E15
B30E05
B30E15
Cylinder Pressure (bar)
Crank Angle (deg)
(b)
D100
B20E05
B20E15
B30E05
B30E15
Heat Release Rate (J/deg)
Crank Angle (deg)

Figure 3

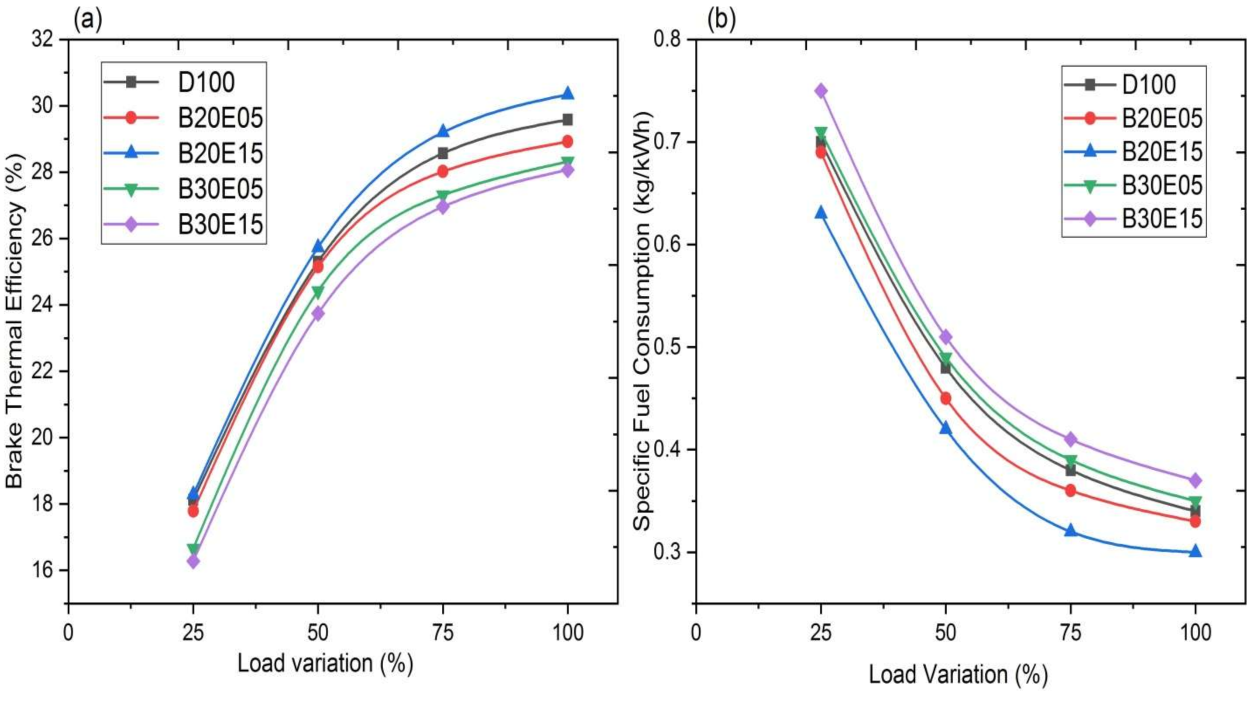
(a)
Brake Thermal Efficiency (%)
Load variation (%)
D100
B20E05
B20E15
B30E05
B30E15
(b)
Specific Fuel Consumption (kg/kWh)
Load Variation (%)
D100
B20E05
B20E15
B30E05
B30E15

Figure 4

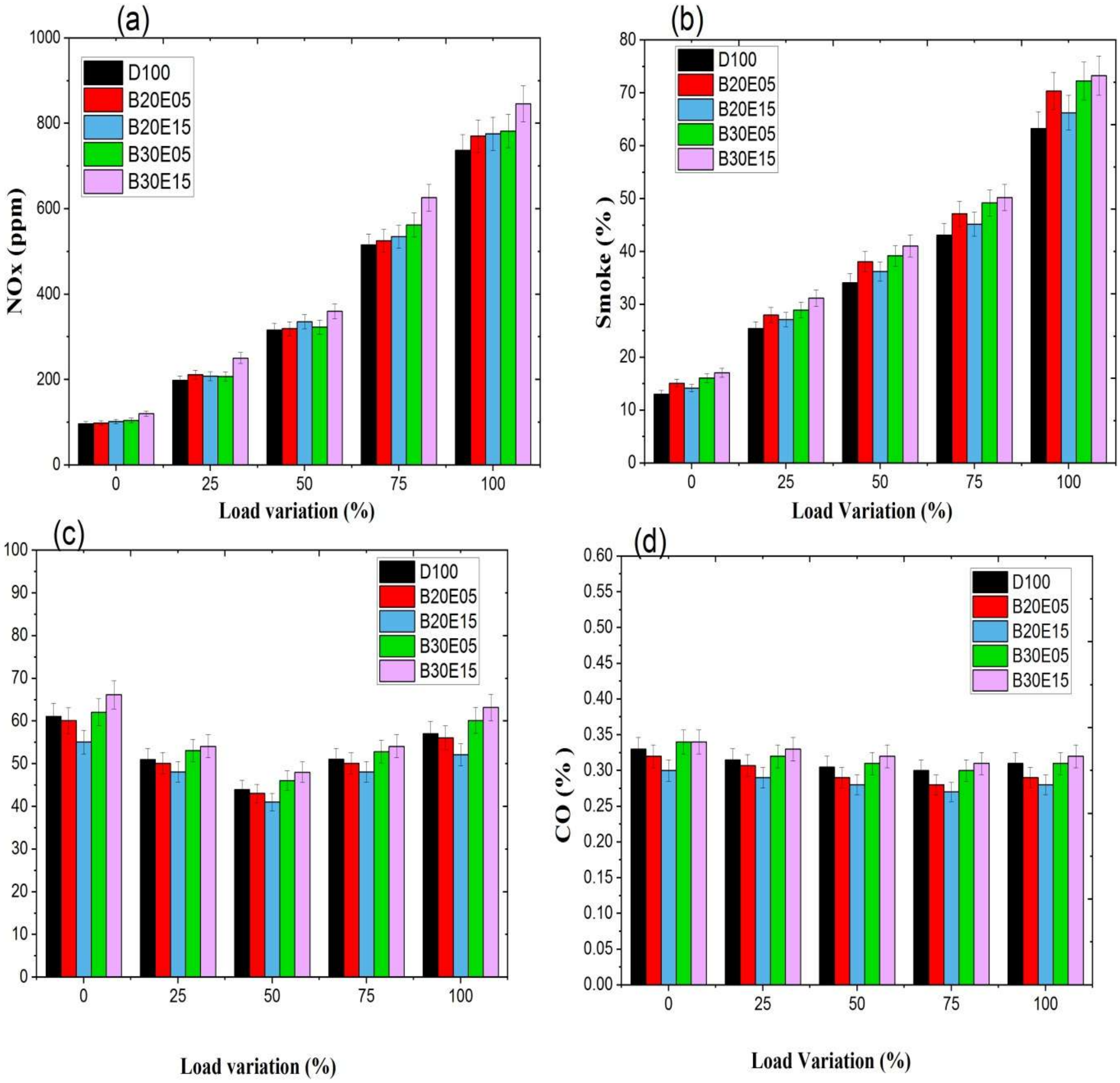
(a)
D100
B20E05
B20E15
B30E05
B30E15
NOx (ppm)
Load variation (%)
(b)
Smoke (%)
Load Variation (%)
(c)
HC (ppm)
Load variation (%)
(d)
CO (%)
Load Variation (%)

Figure 5